Short Communication:

Green Synthesis of Silver Nanoparticles Using *Citrus sinensis* Peels Assisted by Microwave Irradiation as a Contrast Agents for Computed Tomography Imaging

Tanty Fatikasari[1], Iis Nurhasanah[2], and Ali Khumaeni[1,2*]

[1]*Department of Physics, Faculty of Science and Mathematics, Universitas Diponegoro, Jl. Prof. Soedarto SH, Tembalang, Semarang 50275, Indonesia*

[2]*Reseach Center for Laser and Advanced Nanotechnology, Faculty of Science and Mathematics, Universitas Diponegoro, Jl. Prof. Soedharto SH, Tembalang, Semarang 50275, Indonesia*

* ***Corresponding author:***

email: khumaeni@fisika.fsm.undip.ac.id

Received: April 24, 2024
Accepted: June 14, 2024

DOI: 10.22146/ijc.95690

Abstract: *Contrast agents are extensively used to enhance the quality of images in computed tomography (CT) scans for brain exams, vascular imaging, and full-body imaging. Recent data indicate that iodine-based contrast agents have brief durations of blood circulation and may lead to harmful toxicity effects. This study aims to produce silver nanoparticles using environmentally friendly synthesis techniques facilitated by microwaves. The characteristics of nanoparticles have been studied using UV-vis, FTIR, XRD, and TEM techniques. The TEM analysis reveals that the silver nanoparticle has an average diameter of 9 nm and exhibits a spherical shape. The contrast-to-noise ratio (CNR) values of silver nanoparticles at 100, 150, and 200 mg/L concentrations are 35.79, 48.16, and 74.66, respectively. In comparison, iodine exhibits CNR values of 28.57, 34.69, and 48.56 at the same concentrations. The CNR values for tube currents of 140, 160, and 180 mA are 37.83, 44.98, and 48.26, respectively. In contrast, the CNR values in silver nanoparticles are 63.64, 75.32, and 81.67. The results obtained from the different concentrations and tube currents clearly demonstrate that silver nanoparticles have a higher CNR than iopamidol. Hence, silver nanoparticles have significant potential as contrast agents.*

Keywords: *silver nanoparticles; microwave irradiation; contrast agent; computed tomography; contrast-to-noise ratio*

■ INTRODUCTION

Computed tomography (CT) scans are widely used to visualize abnormalities in different human organs [1]. However, it is crucial to recognize that CT scans have certain limitations in distinguishing tissues with identical densities. Therefore, the use of a contrast agent is necessary to augment the quality of photographs. Iodine is often used as a contrast agent in CT scans. Iodine has the capacity to improve picture results; nevertheless, its effectiveness is limited by its short duration of blood circulation [2] and the occurrence of negative effects [3].

Recently, a novel alternative contrast agent called nanoparticles was introduced. High-density metal materials may be used to create effective contrast agents based on nanoparticles. The density of silver, measured at 10.49 g/cm^3, is higher than the density of iodine, which is measured at 4.93 g/cm^3. The increased concentration of silver nanoparticles leads to a greater surface area for interaction, resulting in enhanced absorption of X-rays [4]. In addition, it demonstrates thermal and photostability [4], is cost-effective [5], and can be obtained in a highly pure state [6]. Hence, the utilization of silver nanoparticles holds promise for enhancing medical imaging. According to Mattea et al. [7], the inclusion of silver nanoparticles at various concentrations and depths in the tissue led to an increase in signaling. This finding indicates that silver nanoparticles possess the ability to function as

radiosensitizers and amplifiers of dose. This was clarified by Mondal et al. [8], who used optical coherence tomography (OCT) to view soft tissue in animals. The results indicate that silver nanoparticles can penetrate chicken breast tissue layers, resulting in enhanced contrast and improved imaging depth at different time intervals. Furthermore, nanoparticles have a longer circulation time in the bloodstream compared to iodine, resulting in more accurate imaging [9].

Silver nanoparticles can be synthesized using several methods, including laser ablation, pyrolysis, electron beam lithography, sonochemical processes, and sol-gel processes [10-11]. Nevertheless, this approach is somewhat expensive due to the need for advanced machinery, a large quantity of resources, and its extended duration. A novel method known as green synthesis can address this shortcoming. Green synthesis is a process that involves phytochemical compounds found in plants, such as flavonoids, phenols, tannins, and alkaloids [12-13]. This approach is regarded as ecologically sustainable due to its limited use of chemicals, cost-effectiveness, and reliance on relatively uncomplicated equipment [14-15]. The *Citrus sinensis* peel contains a significant amount of phytochemicals, specifically 15% saponins, 12–14% alkaloids, 3–4% flavonoids, and 3–4% phenols [12]. The phytochemical compound facilitates the transfer of hydroxyl groups, which transfer electrons to silver ions (Ag^+), leading to the reduction and stabilization of silver nanoparticles [16-18]. By repurposing the typically wasted *Citrus sinensis* peel, we can contribute to the reduction of environmental contamination. At room temperature, it can last up to nine months [19]. Because of its storage convenience, it is an ideal candidate for bio-reduction implementation.

We used microwave irradiation to help in synthesizing silver nanoparticles using an extract derived from the peel of *C. sinensis*. The direct interaction between molecular dipoles and electromagnetic waves in microwaves may accelerate the reduction process and generate more uniform heat [14]. An investigation is conducted to analyze the impact of microwave power on the creation of distinct nanoparticles. To determine their properties, the nanoparticles are further analyzed using UV-vis, FTIR, XRD, and TEM techniques. Subsequently, the nanoparticles underwent in vitro testing to evaluate their efficacy as a CT contrast agent. We then compared the obtained findings with those of the standard iodine-based CT contrast agent.

■ EXPERIMENTAL SECTION

Materials

The materials used in this experiment were *C. sinensis* peels, silver nitrate (Merck, 99.8%), sodium hydroxide (NaOH), filtered water, Whatman paper, and iopamidol.

Instrumentation

The tools used were a hotplate stirrer, vacuum filter, Shimadzu UV-1700 UV-vis spectrophotometer, TEM, Samsung microwave operating at a frequency of 2.45 GHz, The FTIR-6300 spectrometer (JASCO, Tokyo, Japan), XRD, microDICOM, and GE 16 slice CT scanner.

Procedure

Citrus sinensis *peel extract preparation*

First, 20 g of *C. sinensis* peels were washed and diced into small pieces before submerging in 200 mL of filtered water. The extract was first immersed and then heated to a temperature of 90 °C for a duration of 10 min. It was then allowed to cool down to the ambient temperature and filtered using Whatman paper. Finally, the extract was thereafter kept in the refrigerator for future use.

Synthesis of silver nanoparticles

A solution containing 0.05 M silver nitrate was combined with 200 mL of peel extracts and adjusted to a pH of 10. The combination was next subjected to microwave irradiation (using a Samsung microwave operating at a frequency of 2.45 GHz) for 5 min, using various power settings (100, 180, 300, 450, and 600 W) to ascertain the most favorable condition. Following the reaction, the liquid underwent a color transformation from a transparent yellow hue to a reddish-brown shade, suggesting the successful synthesis of silver nanoparticles [20-21]. Further, the silver nanoparticle solution is subjected to filtration using a vacuum filter,

resulting in the collection of pellets which are further dried on a hotplate. Subsequently, the powder was collected for further analysis.

Characterization techniques

A UV-vis spectrophotometer was used to maintain the formation of silver nanoparticles in the solution at wavelength 200–700 nm and TEM was used to measure the size of silver nanoparticles. The FTIR spectrum of *C. sinensis* peel extracts and colloidal silver nanoparticles was recorded to investigate how biomolecules act in the formation of silver nanoparticles at wavenumber 4000–500 cm^{-1}, while the crystalline nature was examined by XRD analysis.

In vitro *CT imaging*

Silver nanoparticle powder was dispersed in distilled water at concentrations of 100, 150, and 200 mg/L and then sonicated for 30 min in a 10 mL vial. Iopamidol as iodin-based contrast liquid was also diluted to a similar concentration, which was then homogenized by sonication for 30 min. A GE Revolution Maxima at Primaya Hospital Semarang was used to evaluate *in vitro* CT imaging. With a head procedure slice thickness of 5 mm, the voltage was lowered to its lowest value of 80 kV with varying tube currents of 140–180 mA. The sample is aligned and exposed by the axial method. Following the acquisition of the intensity signal, the data is analyzed using micro-DICOM software to compute the Hounsfield unit (HU) value. HU is taken at the 4 edges of the image, and then the contrast-to-noise ratio (CNR) is calculated using the following Eq. (1) [22];

$$CNR = \frac{P_{object} - P_{background}}{\sqrt{(SD_{object})^2 + (SD_{background})^2}} \quad (1)$$

where P_{object} and $P_{background}$ are the pixel values from ROI in the object and background, while SD are the standard deviation values.

■ RESULTS AND DISCUSSION

Characterization of Synthesized Silver Nanoparticles

UV-vis analysis

The reduction of silver ions into nano-size has been achieved by using microwave irradiation to synthesize silver nanoparticles. Fig. 1 illustrates the color transition from a light-yellow shade to a reddish-brown hue, providing evidence for the creation of silver nanoparticles. To verify the success of the reaction, a UV-vis spectrophotometer was used to observe any color changes in the solutions.

The UV-vis spectra in Fig. 2 demonstrate the surface plasmon resonance of silver nanoparticles, which occurs at wavelengths between 426–472 nm. This phenomenon is a result of the coherent oscillation and vibration of free electrons in the conduction band induced by the input light. The spectral peak response may be seen within the wavelength range of 380 to 400 nm, as shown by earlier studies [17,23]. The graphic demonstrates a positive correlation between power and absorbance, consistent with the findings of Długosz et al. [24]. The silver nanoparticles exhibit 426, 439, 443, 463, and 472 nm

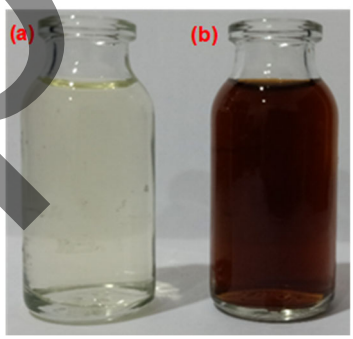

Fig 1. Solution before (a) and after (b) microwave irradiation

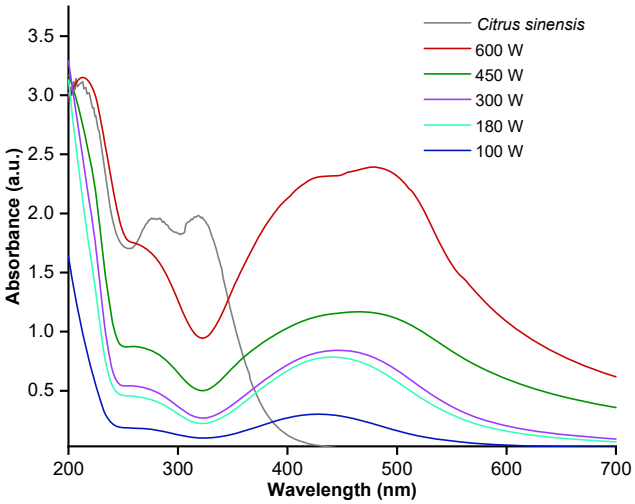

Fig 2. UV-vis spectra of silver nanoparticles synthesized by *Citrus sinensis* peels extract

wavelengths from 100 to 600 W, respectively. The absorbance of the samples shows a positive connection with increasing power. Specifically, the absorbance values are 0.302, 0.785, 0.842, 1.168, and 2.407. Porrawatkul et al. [25] found that higher absorption values indicate a larger number of nanoparticles. Silver nanoparticles have a wavelength range between 400 and 450 nm [17,26]. Wavelengths above 450 nm, which exhibit strong absorption, indicate a higher probability of interparticle interaction and the possibility of particle aggregation in the sample. Consequently, the research determined that a power of 300 W was optimal for synthesizing silver nanoparticles.

FTIR analysis

Fig. 3 displays the FTIR spectra of silver nanoparticles. Fig. 3. shows a comparison of the FTIR spectrum on the colloid of silver nanoparticles with the extract of *C. sinensis* peels. From the spectrum, the groups that play an important role in the reduction process can be analyzed. The presence of O–H bonding, which is a hallmark of a polyphenol molecule, is shown by the absorption peak in the wavenumber range of 3844–3389 cm^{-1} [11]. The peak with the widest spectral width is detected at a wavenumber of 3389 cm^{-1}, which shows a shift towards 3446 cm^{-1}. The process of cluster bonding by oxidation entails breaking the carbon-oxygen bond, creating a carboxylic acid group from a phenolic molecule [25,27]. Zayed et al. [28] reported that the absorption band at 2363 cm^{-1} changed to 2352 cm^{-1}, while the band at 633 cm^{-1} changed to 679 cm^{-1}. The observed changes in wavenumber suggest the existence of carbonyl (C=O) group in the ketones, flavonoids, and terpenoids, thereby demonstrating their chemical reactivity [25,27,29-30].

The absorption peak seen at 1526 cm^{-1} corresponds to the stretching of C=C bond of carbon groups. Alahmad et al. [14] indicated that the absorption band seen at 1382–1405 cm^{-1} is caused by the existence of a C–H bond, as stated by Gurumurthy et al. [31]. The absorption band at 1261 cm^{-1} indicates the presence of flavonoids and catechins [32]. These chemicals later become present in the colloid of silver nanoparticles. The lack of absorbance indicates that this substance is being reduced, emphasizing its crucial contribution to the creation of silver nanoparticles. An absorption band seen at the wavenumbers of 1059–1061 cm^{-1} indicates the presence of a carboxyl group, which may be ascribed to either a C–O–H or C–O–R bond. The investigation done by Rusnaenah et al. [33] found that the presence of silver nanoparticles may be detected by observing the final absorptive tape at 473 cm^{-1}. This discovery aligns with the earlier study conducted by Kokila et al. [29], which stated that silver nanoparticles display a convergence band in the spectral region of 422 to 597 cm^{-1}.

The phytochemical groups responsible for the reduction of silver ions to silver nanoparticles, as shown in Fig. 3, include O–H, C=O, C–H (alkene), C–O (polyol), and C–O–H/C–O–R (carboxyl). These groups are present in phytochemical derivatives referred to as flavonoids, phenols, catechins, terpenoids, and ketones. This research aligns with the studies done by Senthamil et al. [12] and Liew et al. [13], which suggest that the presence of flavonoids and phenols in *C. sinensis* peel extract contributes to the process of reducing silver ions to silver nanoparticles. Furthermore, the component also contributes to the stability of the created silver nanoparticles [34].

XRD analysis

XRD is also used to study the crystalline structure of desiccated silver nanoparticles. The diffraction profile in Fig. 4 displayed four distinct peaks at 2θ values of 38.27,

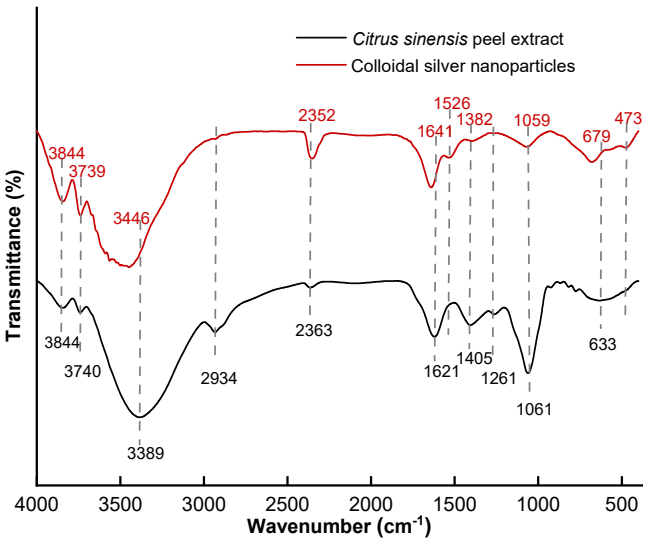

Fig 3. FTIR spectra of silver nanoparticles

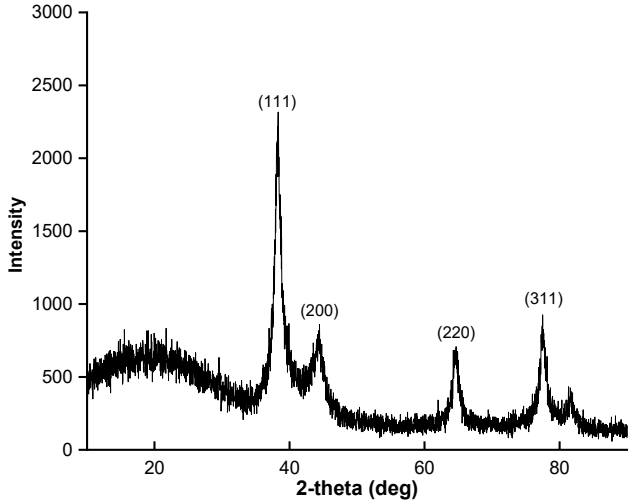

Fig 4. XRD patterns of silver nanoparticles synthesized with *Citrus sinensis* peel extracts

44.21, 64.57, and 77.56°. These peaks correspond to the (111), (200), (220), and (311) crystallographic planes, respectively, according to the standard set by the Joint Committee on Powder Diffraction Standards (JCPDS). This indicates that the synthesized silver nanoparticles possess a face-centered cubic (FCC) crystalline structure [35-36]. Compared to plasmochemical [37] and electrochemical [38] methods, the green synthesis of silver nanoparticles shows a higher intensity, which suggests that there are more nanoparticles [39]. Beyond that, the XRD analysis did not reveal any additional impurities. Furthermore, the green synthesis of silver nanoparticles using *C. sinensis* peel extract assisted by microwaves showed a higher peak than the synthesis conducted at room temperature, despite the use of a lower concentration of silver nitrate.

TEM analysis

TEM is used to analyze the morphology and dimensions of silver nanoparticles. Fig. 5(a) clearly demonstrates that the synthesized nanoparticles exhibit little aggregation. Moreover, the particles have a consistent size distribution and are precisely distributed over the specified region. The histogram shown in Fig. 5(b) shows that the average size of silver nanoparticles is 9 nm, with a range of 3 to 22 nm, and exhibits a spherical form. Compared to previously studied nanoparticles, which ranged from 12 to 41 nm [40-41], the green synthesis of silver nanoparticles has a smaller mean size and a more uniform size distribution [42-43].

Silver Nanoparticles as Contrast for CT Imaging

The nanoparticle powder generated from the experiment is dispersed in an aqueous solution at three specific concentrations (100, 150, and 200 mg/L) and then sonicated. The silver nanoparticle colloids formed were consistently compared to iodine at the same concentration under 80 kV and 160 mA conditions. Fig. 6 illustrates the impact of X-ray radiation on the material. Despite the limited visibility of the color variation in the

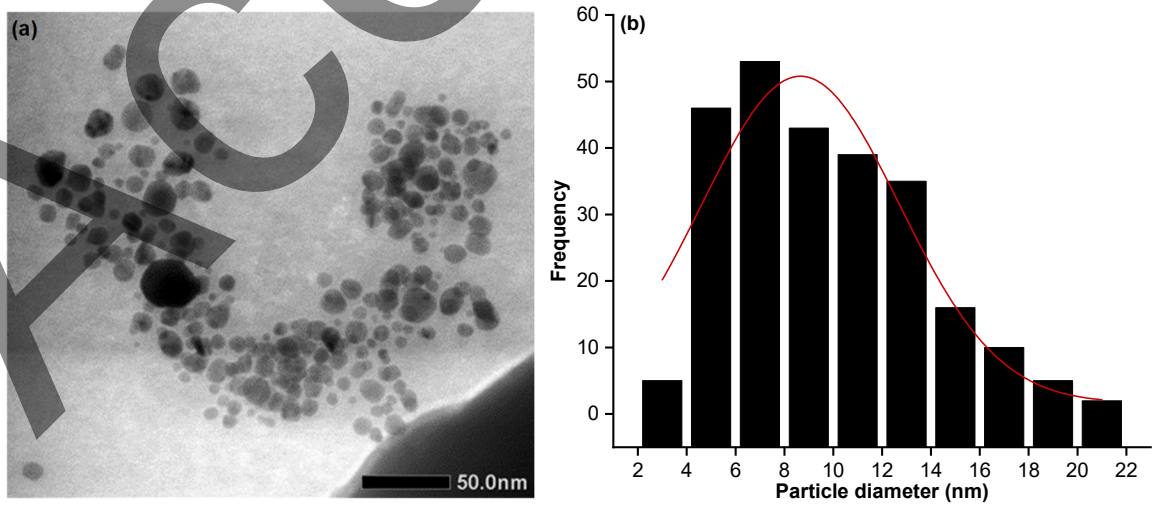

Fig 5. TEM image and size distribution histogram of silver nanoparticles synthesized using *Citrus sinensis* peel extracts assisted by microwave irradiation

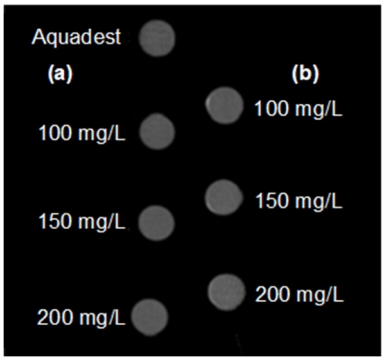

Fig 6. Image results of (a) iopamidol and (b) silver nanoparticles with variations of composition as contrast CT imaging

picture, it is evident that silver nanoparticles produce higher HU values compared to iodine when the average value is calculated.

Fig. 7(a) and 7(b) illustrate the value of silver nanoparticles at various dosages in comparison to iodine. At all concentrations, silver nanoparticles have a higher HU and CNR compared to iodine. The HU values of silver nanoparticles at concentrations of 100, 150, and 200 mg/L are 10.1, 14.6, and 17.6, respectively. In contrast, the HU values of iodine are 6.7, 7.9, and 9.8. The research conducted by Sadeghian et.al. [44] demonstrates that the CNR values exhibit an upward trend as the concentration rises. Consequently, an increase in nanoparticle concentrations will result in a greater absorption of X-rays, thus producing more vivid images [45]. Consistent with the prior investigation, the CNR exhibited a rise in consistency as the concentration increased. The CNR value of silver nanoparticles was 45.48 at a concentration of 100 mg/L, whereas iodine had a CNR value of 35.30. The CNR values for silver nanoparticles at concentrations of 150 and 200 mg/L were 62.83 and 92.85, respectively. In comparison, the CNR values for iodine were 42.94 and 57.82, respectively. With increasing concentrations, the CNR ratio of silver nanoparticles to iodine exhibits an increasing trend, specifically 1.28, 1.48, and 1.6. This is a significant improvement over a study by Sadeghian et al. [44] which discovered a 1.69× increase at a nanoparticle concentration of 2000 mg/L and an energy range of 80–100 keV. This enables the green synthesis of silver nanoparticles to produce greater values as concentrations increase.

The HU values of silver nanoparticles for current variations of 140, 160, and 180 mA are 18.44, 17.56, and 11.4, respectively. In contrast, the HU values of iodine are 10.23, 9.83, and 7.63. Following the computation of CNR values, at the present levels of 140, 160, and 180 mA, the silver nanoparticle values were determined to be 63.64, 75.32, and 81.67, respectively. In contrast, the corresponding values for iodine were found to be 37.83, 44.98, and 48.26. Referring to Fig. 8. As the currents increase, the flow of photons also increases, resulting in better image density. According to the CNR value, increasing density will lead to a reduction in noise,

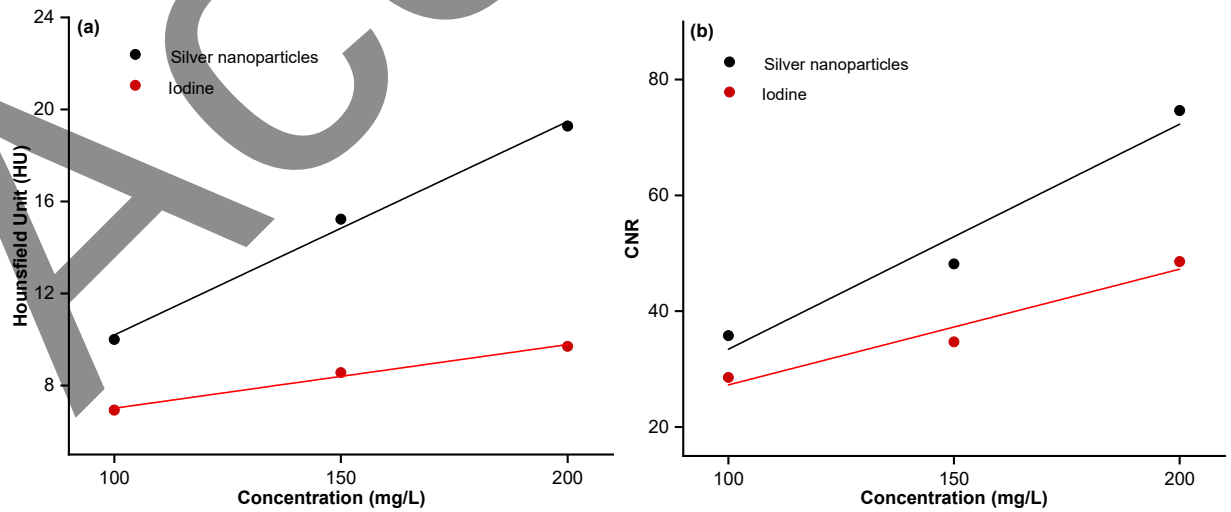

Fig 7. (a) HU of silver nanoparticles and iodine as a function of molar concentration and (b) comparison CNR of silver nanoparticles and iodine at each concentration

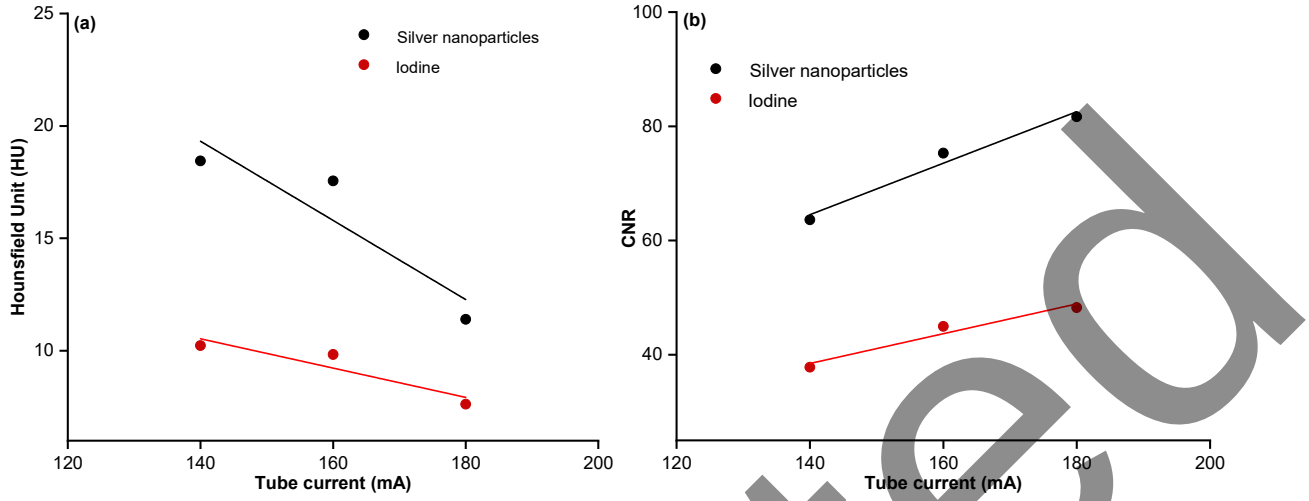

Fig 8. (a) HU of silver nanoparticles and iodine as a function of tube current and (b) Comparison CNR of silver nanoparticles and iodine at each tube current

resulting in enhanced contrast resolution. In addition, a high CNR value signifies a stronger image [46], indicating an improvement in the quality of the CT image. A previous investigation by Matsubara et al. [47] found that increasing the tube current beyond 100 mA led to a substantial decrease in noise. In addition, Katkar et al. [48] also confirmed that an increase in current leads to a corresponding rise in the CNR value.

■ CONCLUSION

Silver nanoparticles were effectively synthesized using *Citrus sinensis* peel extracts, assisted by microwave irradiation for 5 min. The nanoparticles exhibited a spherical morphology, with an average diameter of 9 nm smaller than other methods. The CNR values of silver nanoparticles at concentrations of 100, 150, and 200 mg/L are 35.79, 48.16, and 74.66, respectively. However, iodine exhibits CNR values of 28.57, 34.69, and 48.56 at identical doses. Iodine exhibits CNR values of 37.83, 44.98, and 48.26 at tube currents of 140, 160, and 180 mA, respectively. On the other hand, silver nanoparticles exhibited CNR values of 63.64, 75.32, and 81.67, respectively. The CNR values indicate comparability with the increases in concentration and tube current values. As the concentration and tube current values increase, the picture quality improves. Nanoparticles have shown superior picture quality in comparison to iodine, thereby highlighting their significant potential as a contrast agent.

■ ACKNOWLEDGMENTS

This work was financially supported by Universitas Diponegoro under research grant of *Riset Publikasi Internasional* 2023, No. 569-105/UN7.D2/PP/IV/2023.

■ CONFLICT OF INTEREST

The authors have no conflict of interest.

■ AUTHOR CONTRIBUTIONS

Tanty Fatikasari conducted the experiment and wrote the original manuscript. Iis Nurhasanah designed the methodology. Ali Khumaeni designed concept of experiment, reviewed, and edited the manuscript. All authors agreed to the final version of this manuscript.

■ REFERENCES

[1] Jameel, M.S., Aziz, A.A., Dheyab, M.A., Mehrdel, B., Khaniabadi, P.M., and Khaniabadi, B.M., 2021, Green sonochemical synthesis platinum nanoparticles as a novel contrast agent for computed tomography, *Mater. Today Commun.*, 27, 102480.

[2] Aslan, N., Ceylan, B., Koç, M.M., and Findik, F., 2020, Metallic nanoparticles as X-ray computed tomography (CT) contrast agents: A review, *J. Mol. Struct.*, 1219, 128599.

[3] Caro, C., Dalmases, M., Figuerola, A., García-Martín, M.L., and Leal, M.P., 2017, Highly water-stable rare ternary Ag-Au-Se nanocomposites as

long blood circulation time X-ray computed tomography contrast agents, *Nanoscale*, 9 (21), 7242–7251.

[4] Lee, S.H., and Jun, B.H., 2019, Silver nanoparticles: Synthesis and application for nanomedicine, *Int. J. Mol. Sci*., 20 (4), 865.

[5] Patel, S., and Patel, N.K., 2021, A Review on synthesis of silver nanoparticles - A green expertise, *Life Sci. Leafl.*, 132, 16–24.

[6] Abdulwahid, T.A., and Abid Ali, I.J., 2019, Investigation the effect of silver nanoparticles on sensitivity enhancement ratio in improvement of adipose tissue radiotherapy using high energy photons, *IOP Conf. Ser.: Mater. Sci. Eng.*, 571 (1), 012108.

[7] Mattea, F., Vedelago, J., Malano, F., Gomez, C., Strumia, M.C., and Valente, M., 2017, Silver nanoparticles in X-ray biomedical applications, *Radiat. Phys. Chem.*, 130, 442–450.

[8] Mondal, I., Raj, S., Roy, P., and Poddar, R., 2018, Silver nanoparticles (AgNPs) as a contrast agent for imaging of animal tissue using swept-source optical coherence tomography (SSOCT), *Laser Phys.*, 28 (1), 015601.

[9] Fedorenko, S.V., Grechkina, S.L., Mukhametshina, A.R., Solovieva, A.O., Pozmogova, T.N., Miroshnichenko, S.M., Alekseev, A.Y., Shestopalov, M.A., Kholin, K.V., Nizameev, I.R., and Mustafina, A.R., 2018, Silica nanoparticles with Tb(III)-centered luminescence decorated by Ag^0 as efficient cellular contrast agent with anticancer effect, *J. Inorg. Biochem*., 182, 170–176.

[10] Salnus, S., Wahab, W., Arfah, R., Zenta, F., Natsir, H., Muriyati, M., Fatimah, F., Rajab, A., Armah, Z., and Irfandi, R., 2022, A review on green synthesis, antimicrobial applications and toxicity of silver nanoparticles mediated by plant extract, *Indones. J. Chem.*, 22 (4), 1129–1143.

[11] Gautam, D., Dolma, K.G., Khandelwal, B., Gupta, M., Singh, M., Mahboob, T., Teotia, A., Thota, P., Bhattacharya, J., Goyal, R., Oliveira, S.M.R., Pereira, M.L., Wiart, C., Wilairatana, P., Eawsakul, K., Rahmatullah, M., Saravanabhavan, S.S., and Nissapatorn, V., 2023, Green synthesis of silver nanoparticles using *Ocimum sanctum* Linn. and its antibacterial activity against multidrug resistant *Acinetobacter baumannii*, *PeerJ*, 11, e15590.

[12] Senthamil S.R., Anish Kumar, R.Z., and Bhaskar, A., 2016, Phytochemical investigation and *in vitro* antioxidant activity of *Citrus sinensis* peel extract, *Pharm. Lett.*, 8 (3), 159–165.

[13] Liew, S.S., Ho, W.Y., Yeap, S.K., and Bin Sharifudin, S.A., 2018, Phytochemical composition and *in vitro* antioxidant activities of *Citrus sinensis* peel extracts, *PeerJ*, 6, e5331.

[14] Alahmad, A., Al-Zereini, W.A., Hijazin, T.J., Al-Madanat, O.Y., Alghoraibi, I., Al-Qaralleh, O., Al-Qaraleh, S., Feldhoff, A., Walter, J.G., and Scheper, T., 2022, Green synthesis of silver nanoparticles using *Hypericum perforatum* L. aqueous extract with the evaluation of its antibacterial activity against clinical and food pathogens, *Pharmaceutics*, 14 (5), 1104.

[15] Oves, M., Ahmar Rauf, M., Aslam, M., Qari, H.A., Sonbol, H., Ahmad, I., Sarwar Zaman, G., and Saeed, M., 2022, Green synthesis of silver nanoparticles by *Conocarpus lancifolius* plant extract and their antimicrobial and anticancer activities, *Saudi J. Biol. Sci.*, 29 (1), 460–471.

[16] Sharma, L., Dhiman, M., Singh, A., and Sharma, M.M., 2021, Biological synthesis of silver nanoparticles using *Nyctanthes arbor-tristis* L.: A green approach to evaluate antimicrobial activities, *Mater. Today: Proc.*, 43, 2915–2920.

[17] Lai, X., Guo, R., Xiao, H., Lan, J., Jiang, S., Cui, C., and Ren, E., 2019, Rapid microwave-assisted bio-synthesized silver/dandelion catalyst with superior catalytic performance for dyes degradation, *J. Hazard. Mater.*, 371, 506–512.

[18] Simatupang, C., Jindal, V.K., and Jindal, R., 2021, Biosynthesis of silver nanoparticles using orange peel extract for application in catalytic degradation of methylene blue dye, *Environ. Nat. Resour. J.*, 19 (6), 468–480.

[19] Khammar, Z., Sadeghi, E., Raesi, S., Mohammadi, R., Dadvar, A., and Rouhi, M., 2022, Optimization of biosynthesis of stabilized silver nanoparticles

using bitter orange peel by-products and glycerol, *Biocatal. Agric. Biotechnol.*, 43, 102425.

[20] Rohaeti, E., and Rakhmawati, A., 2017, Application of *Terminalia catappa* in preparation of silver nanoparticles to develop antibacterial nylon, *Orient. J. Chem*., 33 (6), 2905–2912.

[21] Deivanathan, S.K., and Prakash, J.T.J., 2022, Green synthesis of silver nanoparticles using aqueous leaf extract of *Guettarda speciosa* and its antimicrobial and anti-oxidative properties, *Chem. Data Collect.*, 38, 100831.

[22] Davis, A.T., Palmer, A.L., Pani, S., and Nisbet, A., 2018, Assessment of the variation in CT scanner performance (image quality and Hounsfield units) with scan parameters, for image optimisation in radiotherapy treatment planning, *Physica Med.*, 45, 59–64.

[23] Drummer, S., Madzimbamuto, T., and Chowdhury, M., 2021, Green synthesis of transition metal nanoparticles and their oxides: A review, *Materials*, 14 (11), 2700.

[24] Długosz, O., and Banach, M., 2020, Continuous synthesis of metal and metal oxide nanoparticles in microwave reactor, *Colloids Surf., A*, 606, 125453.

[25] Porrawatkul, P., Pimsen, R., Kuyyogsuy, A., Teppaya, N., Noypha, A., Chanthai, S., and Nuengmatcha, P., 2022, Microwave-assisted synthesis of Ag/ZnO nanoparticles using *Averrhoa carambola* fruit extract as the reducing agent and their application in cotton fabrics with antibacterial and UV-protection properties, *RSC Adv.*, 12 (24), 15008–15019.

[26] Mogole, L., Omwoyo, W., Viljoen, E., and Moloto, M., 2021, Green synthesis of silver nanoparticles using aqueous extract of *Citrus sinensis* peels and evaluation of their antibacterial efficacy, *Green Process. Synth.*, 10 (1), 851–859.

[27] Kummara, S., Patil, M.B., and Uriah, T., 2016, Synthesis, characterization, biocompatible and anticancer activity of green and chemically synthesized silver nanoparticles – A comparative study, *Biomed. Pharmacother.*, 84, 10–21.

[28] Zayed, M., Ghazal, H., Othman, H.A., and Hassabo, A.G., 2021, Synthesis of different nanometals using *Citrus sinensis* peel (orange peel) waste extraction for valuable functionalization of cotton fabric, *Chem. Pap.*, 76 (2), 639–660.

[29] Kokila, T., Ramesh, P.S., and Geetha, D., 2015, Biosynthesis of silver nanoparticles from Cavendish banana peel extract and its antibacterial and free radical scavenging assay: A novel biological approach, *Appl. Nanosci.*, 5 (8), 911–920.

[30] Adrianto, N., Panre, A.M., Istiqomah, N.I., Riswan, M., Apriliani, F., and Suharyadi, E., 2022, Localized surface plasmon resonance properties of green synthesized silver nanoparticles, *Nano-Struct. Nano-Objects*, 31, 100895.

[31] Gurumurthy, B.R., Dinesh, B., and Ramesh, K.P., 2017, Structural analysis of merino wool, pashmina and angora fibers using analytical instruments like scanning electron microscope and infra-red spectroscopy, *Int. J. Eng. Technol. Sci. Res.*, 4 (8), 112–125.

[32] Rengga, W.D.P., Yufitasari, A., and Adi, W., 2017, Synthesis of silver nanoparticles from silver nitrate solution using green tea extract (*Camelia sinensis*) as bioreductor, *JBAT*, 6 (1), 32–38.

[33] Rusnaenah, A., Zakir, M., and Budi, P., 2017, Synthesis of silver nanoparticles using bioreductor of catappa leaf extract (*Terminalia catappa*), *Indones. Chim. Acta*, 10 (1), 35–43.

[34] Bawazeer, S., Rauf, A., Shah, S.U.A., Shawky, A.M., Al-Awthan, Y.S., Bahattab, O.S., Uddin, G., Sabir, J., and El-Esawi, M.A., 2021, Green synthesis of silver nanoparticles using *Tropaeolum majus*: Phytochemical screening and antibacterial studies, *Green Process. Synth.*, 10 (1), 85–94.

[35] Nnemeka, I., Godwin, E.U., Olakunle, F., Olushola, O., Moses, O., Chidozie, O.P., and Rufus, S., 2016, Microwave enhanced synthesis of silver nanoparticles using orange peel extracts from Nigeria, *Chem. Biomol. Eng.*, 1 (1), 5–11.

[36] Susan Punnoose, M., Bijimol, D., and Mathew, B., 2021, Microwave assisted green synthesis of gold nanoparticles for catalytic degradation of environmental pollutants, *Environ. Nanotechnol., Monit. Manage.*, 16, 100525.

[37] Skiba, M.I., and Vorobyova, V.I., 2019, Synthesis of silver nanoparticles using orange peel extract prepared by plasmochemical extraction method and degradation of methylene blue under solar irradiation, *Adv. Mater. Sci. Eng.*, 2019 (1), 8306015.

[38] Sabzi, M., and Mersagh Dezfuli, S., 2018, A study on the effect of compositing silver oxide nanoparticles by carbon on the electrochemical behavior and electronic properties of zinc-silver oxide batteries, *Int. J. Appl. Ceram. Technol.*, 15 (6), 1446–1458.

[39] Badi'ah, H.I., Seedeh, F., Supriyanto, G., and Zaidan, A.H., 2019, Synthesis of silver nanoparticles and the development in analysis method, *IOP Conf. Ser.: Earth Environ. Sci.*, 217 (1), 012005.

[40] Hassan, A.M.S., Mahmoud, A.B.S., Ramadan, M.F., and Eissa, M.A., 2022, Microwave-assisted green synthesis of silver nanoparticles using *Annona squamosa* peels extract: Characterization, antioxidant, and amylase inhibition activities, *Rend. Lincei Sci. Fis. Nat.*, 33 (1), 83–91.

[41] Horne, J., De Bleye, C., Lebrun, P., Kemik, K., Van Laethem, T., Sacré, P.Y., Hubert, P., Hubert, C., and Ziemons, E., 2023, Optimization of silver nanoparticles synthesis by chemical reduction to enhance SERS quantitative performances: Early characterization using the quality by design approach, *J. Pharm. Biomed. Anal.*, 233, 115475.

[42] Lokman, M.Q., Mohd Rusdi, M.F., Rosol, A.H.A., Ahmad, F., Shafie, S., Yahaya, H., Mohd Rosnan, R., Abdul Rahman, M.A., and Harun, S.W., 2021, Synthesis of silver nanoparticles using chemical reduction techniques for Q-switcher at 1.5 μm region, *Optik*, 244, 167621.

[43] Mamdouh, S., Mahmoud, A., Samir, A., Mobarak, M., and Mohamed, T., 2022, Using femtosecond laser pulses to investigate the nonlinear optical properties of silver nanoparticles colloids in distilled water synthesized by laser ablation, *Physica B*, 631, 413727.

[44] Sadeghian, M., Akhlaghi, P., and Mesbahi, A., 2020, Investigation of imaging properties of novel contrast agents based on gold, silver and bismuth nanoparticles in spectral computed tomography using Monte Carlo simulation, *Pol. J. Med. Phys. Eng.*, 26 (1), 21–29.

[45] Xue, N.C., Zhou, C.H., Chu, Z.Y., Chen, L.N., and Jia, N.Q., 2021, Barley leaves mediated biosynthesis of Au nanomaterials as a potential contrast agent for computed tomography imaging, *Sci. China: Technol. Sci.*, 64 (2), 433–440.

[46] Dance, D.R., Christofides, S., Maidment, A.D.A., McLean, I.D., and Ng, K.H., 2014, *Diagnostic Radiology Physics: A Handbook for Teachers and Students*, International Atomic Energy Agency, Vienna, Austria.

[47] Matsubara, K., Takata, T., Kobayashi, M., Kobayashi, S., Koshida, K., and Gabata, T., 2016, Tube current modulation between single-and dual-energy CT with a second-generation dual-source scanner: Radiation dose and image quality, *Am. J. Roentgenol.*, 207 (2), 354–361.

[48] Katkar, R., Steffy, D.D., Noujeim, M., Deahl, S.T., and Geha, H., 2016, The effect of milliamperage, number of basis images, and export slice thickness on contrast-to-noise ratio and detection of mandibular canal on cone beam computed tomography scans: An *in vitro* study, *Oral Surg., Oral Med., Oral Pathol., Oral Radiol.*, 122 (5), 646–653.